The Fifth International Conference on Railway Technology
RAILWAYS 2022
22–25 August 2022
Montpellier, France

Proceedings of the Fifth International Conference on
Railway Technology:
Research, Development and Maintenance
Edited by J. Pombo
Civil-Comp Conferences, Volume 1, Paper 34.5
Civil-Comp Press, Edinburgh, United Kingdom, 2022, doi: 10.4203/ccc.1.34.5
©Civil-Comp Ltd, Edinburgh, UK, 2022

Study on crashworthiness of concave polygonal tubes evolved from two approaches

Jing Zhang [1,2,3], Suchao Xie[1,2,3], Zinan Liu[1,2,3], Shiwei Zheng[1,2,3]

[1] Key Laboratory of Traffic Safety on Track (Central South University), Ministry of Education, Changsha, Hunan, China
[2] Joint International Research Laboratory of Key Technology for Rail Traffic Safety, Changsha, Hunan, China
[3]National & Local Joint Engineering Research Centre of Safety Technology for Rail Vehicle, Changsha, Hunan, China

Abstract

Aiming at the limited energy absorption (EA) of traditional thin-walled structures, the crashworthiness of concave polygonal tubes evolved from convex polygonal tubes is studied. Based on the first evolution proposed by most scholars, another evolution is put forward. The results show that under the same mass, the EA characteristic of the polygonal tubes with concave angle is improved obviously, and the EA characteristic of approach II is more outstanding. In addition, the theoretical analysis of the mean crushing force (MCF) of concave tubes is deduced by using the simplified super folding element theory.

Keywords: crashworthiness, concave tubes, theoretical analysis.

1 Introduction

Thin-walled structure, as an efficient energy-absorbing element, has been widely used in transportation, industrial manufacturing, and aerospace due to the advantages of its excellent energy dissipation capacity, low cost, and easy installation.

The crashworthiness of thin-walled structures is affected by many factors, such as cross-section shape, effective length, wall thickness, material properties, load conditions, etc. In the past decades, studies on various cross-sectional structures, such as circles, squares, hexagons, octagons, etc., have shown that the most severe plastic deformation occurs near the corners of thin-walled tubes, which contributes to the

dissipation of large amounts of energy, including bending deformation and membrane deformation. Therefore, the number of angles determines the EA and crashworthiness.

One of the defects of traditional thin-walled structures is limited EA and large load fluctuation. Increasing the number of edges of a convex polygonal tube is an effective way to improve the EA characteristic, but the crushing force will reach a saturated state when the number of edges increases to more than 11[1]. To overcome the defect, researchers began to study the EA characteristics of the concave tubes. Reddy et al.[2] introduced extra stability angle on square tube to improve the EA efficiency and 12-side section has significant advantages, which was applied to the simulation of full-vehicle crash test. A new type of thin-walled tube[3] with concave angles is proposed to improve the crashworthiness performance of the traditional hexagonal thin-walled tube. In addition, star-shaped tubes[4], hierarchical concave tubes[5], and circumferentially corrugated tubes[6] have been proposed and studied by many researchers.

So far, most researchers have introduced concave angles to convex polygonal tubes (Figure 1(a)) with individual sectional shapes. This common evolution method (Figure 1(b)) can improve the crashworthiness to a certain extent, but the evolution method is single. Therefore, the EA characteristics of concave tubes under quasi-static compression evolved from N-polygons need to be systematically studied and summarized. New evolutionary methods are developed to compare and improve the EA characteristics of thin-walled structures (Figure 1(c)). All the thin-walled tubes are of the same mass.

It should be noted that, for convenience, ‘Q’, ’P’, and ’H’ denote quadrilateral, pentagonal, and hexagon respectively. ‘TW’ and ‘CT’ denote thin-walled tubes and concave tubes. ‘A’ and ‘E’ represent angular and edge indented from convex polygon tubes respectively.

2 Methods

The crashworthiness of thin-walled structures is often evaluated using appropriate indicators. Generally, indicators, such as EA, specific energy absorption(SEA), initial peak crushing force(IPCF), MCF, and crushing force efficiency (CFE) are introduced to assess the crashworthiness [7].

Quasi-static axial compression of the structure was numerically simulated by using the finite element explicit software LS-DYNA. The thin-walled tubes with length L of 200mm, thickness t of 1.3mm. AA6061-O materials were used for tubes. Literature data have been used to validate the FE models (Figure 2(a)) to be used in the study. Sun et al. [8]have carried out experiments for Q_TW and Q_CT-A under quasi-static compression, and more details can be found in the research. The FE model with the same test specimen configuration is modeled. The deformation patterns of Q_TW and Q_CT-A at corresponding stages of experiments and FE simulation are presented in Figure 2(b). Both Q_TW and Q_CT-A present progressive folding deformation. For Q_CT-A, ten folds are formed in both test and simulation, corresponding to ten

fluctuation cycles on the force-displacement curve. The force-displacement curves obtained by FE simulation and experiments are given in Figure 3. The results show that the test and simulation curves of Q_TW and Q_CT-A follow similar trends, and wave peaks and throughs are in good agreement. And, the comparisons between the FE results and the test values of SEA, IPCF, and MCF are given in Table 1. All the deviations are less than 4%, which indicates that simulation results agree well with the test results. The results show that the FE model is feasible and can be utilized to analyze the crashworthiness of concave tubes under quasi-static compression.

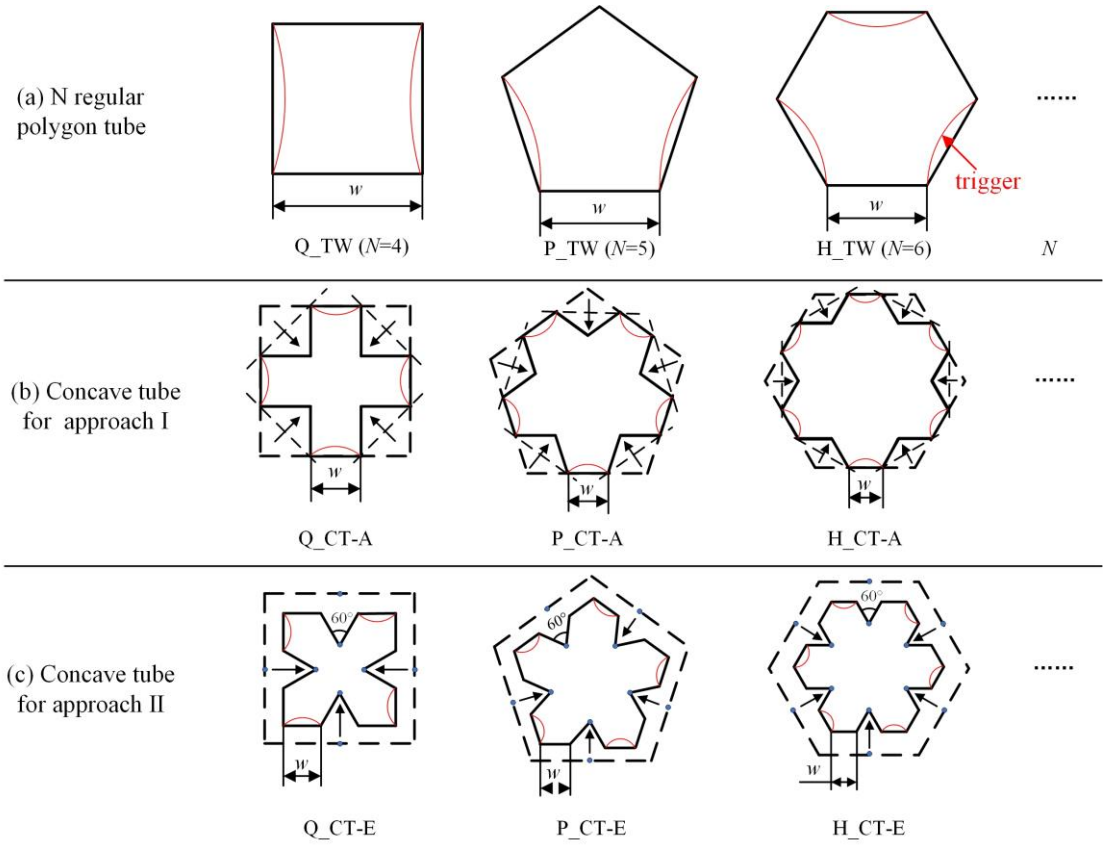

Figure 1: Geometric structure (a) N-regular polygon tube; (b) Concave tube for approach I; (c) Concave tube for approach II.

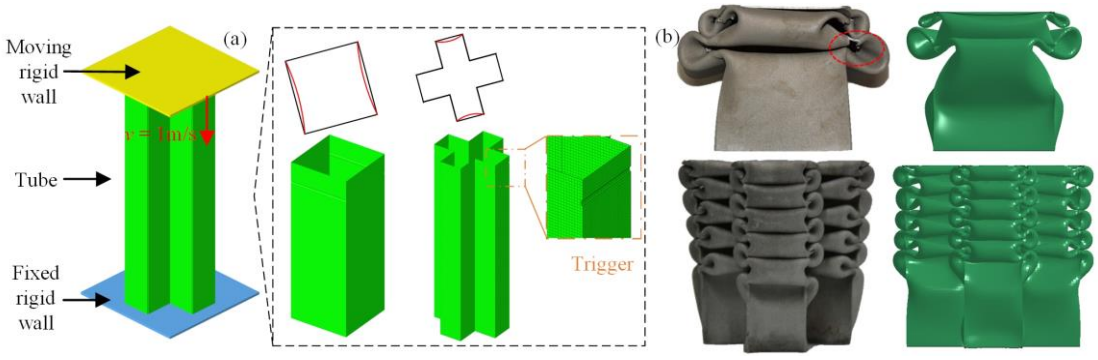

Figure 2: (a) FE models; (b) Comparison of the deformation modes of the test[8] and FE simulation.

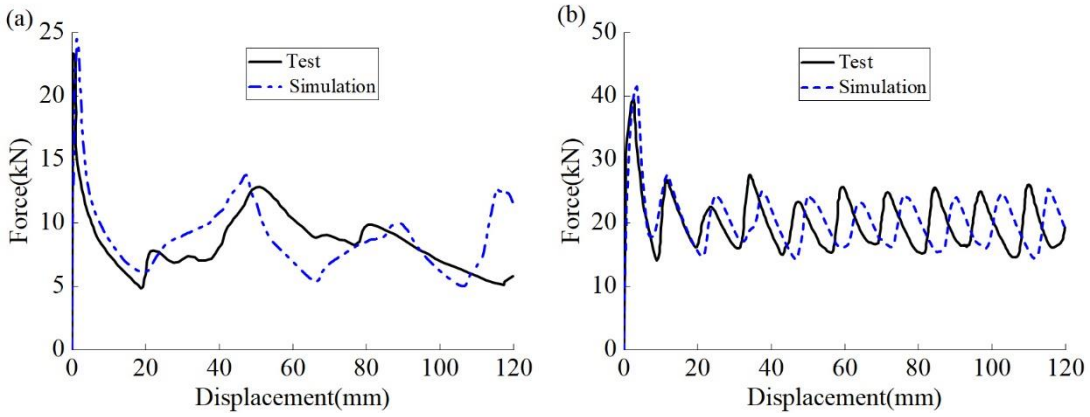

Figure 3: Comparison of the test[8] and FE simulation force-displacement curves: (a) Q_TW; (b) Q_CT-A.

Structure	Type	M [Kg]	SEA [KJ/Kg]	IPCF [KN]	MCF [KN]
Q_TW	Test	0.201	5.11	23.35	8.58
	Simulation	0.201	5.30	23.99	8.88
	Error	0.01%	3.72%	2.74%	3.50%
Q_CT-A	Test	0.201	12.58	41.07	21.10
	Simulation	0.201	12.24	41.75	20.51
	Error	0%	2.70%	1.65%	2.80%

Table 1: Comparison of the test[8] and FE simulation results

3 Results

The first folding flange comes from the trigger, and most of the tubes show progressive folding deformation (Figure 4).

The force-displacement curves of concave tubes (Figure 5(a)) are all distributed above the regular polygon tubes (Figure 5(b)), and the total EA is about 2 to 3 times as much as that of the regular polygon tubes (Table 2). Moreover, P_CT-A has the highest EA because more serious bending deformation and membrane deformation occur near the angle, and the EA performance of approach I is better than approach II.

The simplified super folding element theory proposed by Chen et al.[9] is evaluated through theoretical analysis. The sum of energy dissipation of bending (Figure 6(a)-(b)) and membrane deformation (Figure 6(c)) is equal to external work, which can be expressed as follows,

$$F_m \cdot 2H \cdot \eta = W_{bending} + W_{membrane} \tag{1}$$

F_m represents MCF, η is the coefficient of effective crushing distance.

The bending energy in a folding wavelength can be expressed as

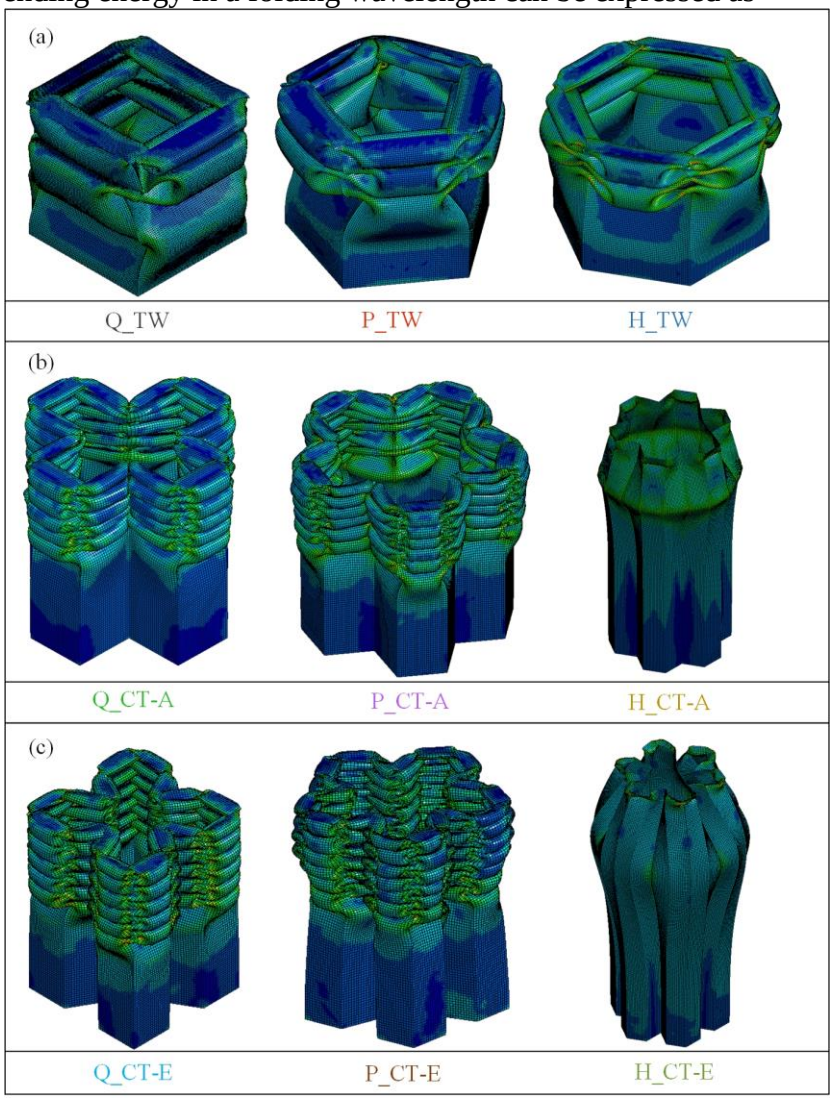

Figure 4: Deformation diagram (a) Regular polygon tube; (b) Concave tube for approach I; (c) Concave tube for approach II.

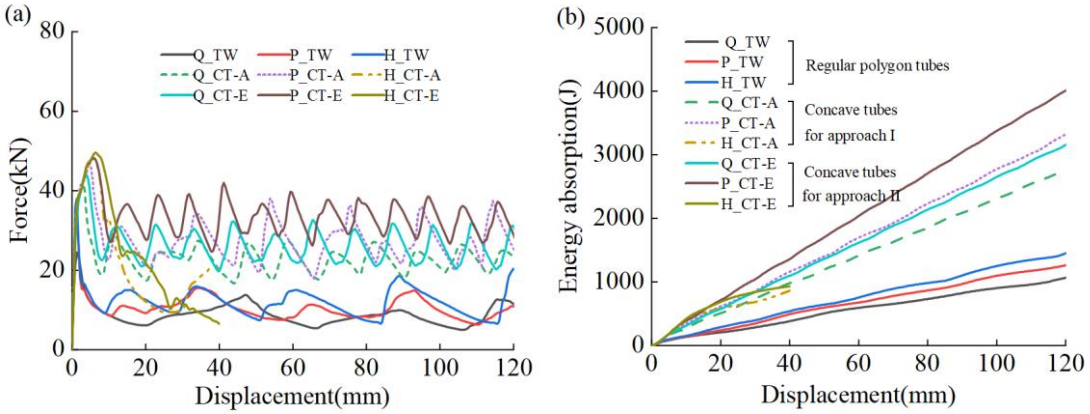

Figure 5: (a) Force-displacement curve; (b) energy absorption-displacement curve

Structure	Type	M [g]	EA [J]	SEA [J/g]	IPCF [KN]	MCF [KN]	CFE
Regular polygon tubes	Q_TW	201	1065.45	5.30	23.99	8.88	0.37
	P_TW	201	1261.75	6.28	26.71	10.51	0.39
	H_TW	201	1449.31	7.21	38.07	12.08	0.32
Concave tubes for approach I	Q_CT-A	201	2767.50	13.77	41.75	23.06	0.55
	P_CT-A	201	3316.56	16.50	47.17	27.64	0.59
	H_CT-A	201	862.48	4.29	48.08	7.19	0.15
Concave tubes for approach II	Q_CT-E	201	3152.85	15.69	44.11	26.27	0.60
	P_CT-E	**201**	**4006.71**	**19.93**	**48.24**	**33.39**	**0.69**
	H_CT-E	201	931.74	4.64	49.62	7.76	0.16

Table 2: Crashworthiness indicators of regular polygon tubes and concave tubes

$$W_{bending} = \sum_{i=1}^{n} M_0 \varphi_i w = 2\pi M_0 w, M_0 = \frac{1}{4}\sigma_0 t^2 \quad (2)$$

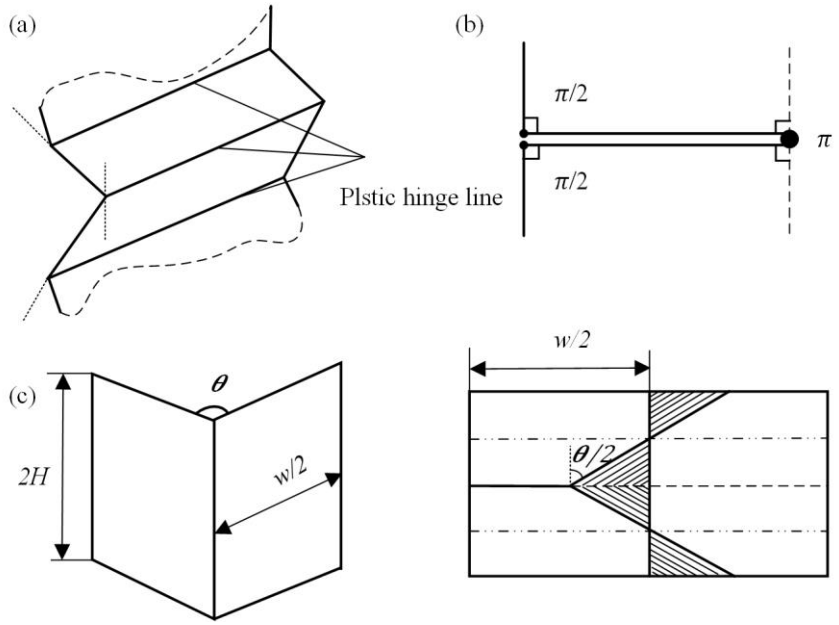

Figure 6: Deformation diagram (a) Bending hinge lines; (b) Rotation angle; (c) Membrane deformation.

Where, σ_0 represents the equivalent plastic flow stress.

$$\sigma_0 = \sqrt{\frac{\sigma_y \sigma_u}{n+1}} \quad (3)$$

n is the power law exponent, for concave tubes derived from N-side, the inner angle of regular *N* polygon is

$$\alpha = \frac{N-2}{N} \cdot 180^{\circ} \tag{4}$$

Zhang et al.[10] combined the membrane deformation energy (Fig. 6 (c)) and obtained the following calculation formula:

$$W_{membrane}^{corner} = \int_s \sigma_0 t ds = \frac{4M_0 H^2 \tan(\alpha/2)}{(\tan(\alpha/2) + 0.05/\tan(\alpha/2))t/1.1} \tag{5}$$

The concave tube structure is decomposed (Figure.7) and the energy conservation formulas of approach I and approach II can be expressed respectively as

$$F_{m\mathrm{I}} \cdot 2H \cdot \eta = 3NW_{bending} + 3NW_{membrane} \tag{6}$$

$$F_{m\Pi} \cdot 2H_{\Pi} \cdot \eta = 4NW_{bending} + NW_{membrane}^{cv1} + 2NW_{membrane}^{cv2} + NW_{membrane}^{cc} \tag{7}$$

The H can be determined by the stationary condition of the MCF,

$$\frac{\partial F_m}{\partial H} = 0 \tag{8}$$

So,

$$H_{\mathrm{I}} = \sqrt{\frac{\pi t w}{2k_{\mathrm{I}}}}, k_{\mathrm{I}} = \frac{1.1\tan(\alpha/2)}{\tan(\alpha/2) + 0.05/\tan(\alpha/2)} \tag{9}$$

$$\begin{aligned} H_{\Pi} &= \sqrt{\frac{2\pi t w}{k_{\Pi}}}, k_{\Pi} = k_{\Pi}^{'} + 2k_{\Pi}^{''} + k_{\Pi}^{'''} \\ k_{\Pi}^{'} &= \frac{1.1\tan(\alpha/2)}{\tan(\alpha/2) + 0.05/\tan(\alpha/2)}, \\ k_{\Pi}^{''} &= \frac{1.1\tan(120^{\circ}/2)}{\tan(120^{\circ}/2) + 0.05/\tan(120^{\circ}/2)} = \frac{61}{60}, \\ k_{\Pi}^{'''} &= \frac{1.1\tan(60^{\circ}/2)}{\tan(60^{\circ}/2) + 0.05/\tan(60^{\circ}/2)} = \frac{2}{5} \end{aligned} \tag{10}$$

The MCF of concave tubes can be obtained,

$$F_{m\mathrm{I}} = \frac{3N}{2\eta}\sqrt{2k_{\mathrm{I}}\pi}\sigma_0 t^{\frac{3}{2}} w^{\frac{1}{2}} \tag{11}$$

$$F_{m\Pi} = \frac{2N}{\eta}\sqrt{\frac{k_{\Pi}\pi}{2}}\sigma_0 t^{\frac{3}{2}} w^{\frac{1}{2}} \tag{12}$$

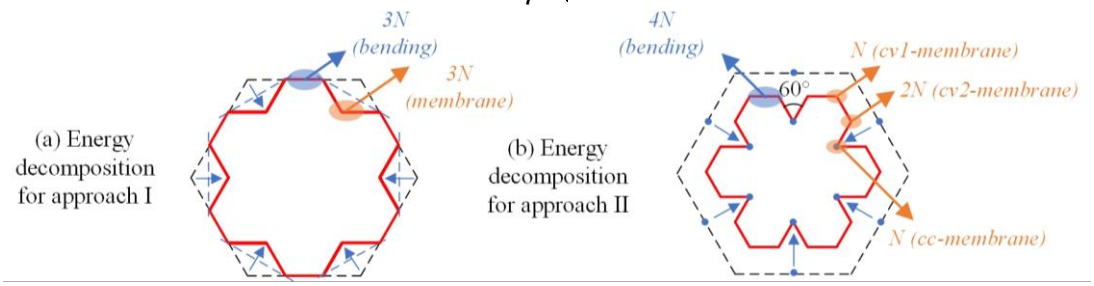

Figure 7: Energy decomposition for (a) Approach I; (b) Approach II.

4 Conclusions and Contributions

In this paper, the crashworthiness of the traditional polygonal thin-walled tubes and the concave tubes evolved from two approaches were studied. The results show that the EA characteristic of the concave tubes is improved obviously, and the highest EA is P_CT-A. Except for H_CT-A and H_CT-E tubes, the other thin-walled tubes produced progressive folding modes with high EA efficiency. Generally speaking, the concave tubes form more lobes and smaller folding wavelengths than those of the TW. Because more serious bending deformation and membrane deformation occur near the angle, the EA performance of approach II is better than approach I.

The theoretical MCF of concave polygonal tubes under two approaches is deduced by the simplified super folded element theory. The MCF of the concave tubes evolved from the traditional regular polygon is systematically summarized. The reasons for the improvement of EA characteristics of concave polygonal tubes in the two approaches are explained from the mechanism, and the new approach II has more advantages.

References

[1] Yamashita M, Gotoh M, Sawairi Y. Axial crush of hollow cylindrical structures with various polygonal cross-sections: Numerical simulation and experiment [J]. Journal of Materials Processing Technology, 2003, 140(1): 59-64.

[2] Reddy S, Abbasi M, Fard M. Multi-cornered thin-walled sheet metal members for enhanced crashworthiness and occupant protection [J]. Thin-Walled Structures, 2015, 94: 56-66.

[3] Chen J, Li E, Li Q, et al. Crashworthiness and optimization of novel concave thin-walled tubes [J]. Composite Structures, 2022, 283:115109.

[4] Deng X, Liu W, Lin Z. Experimental and theoretical study on crashworthiness of star-shaped tubes under axial compression [J]. Thin-Walled Structures, 2018, 130: 321-31.

[5] Li Y, You Z. Origami concave tubes for energy absorption [J]. International Journal of Solids and Structures, 2019, 169: 21-40.

[6] Albak E İ. Crashworthiness design and optimization of nested structures with a circumferentially corrugated circular outer wall and inner ribs [J]. Thin-Walled Structures, 2021, 167:108219.

[7] Ma W, Li Z, Xie S. Crashworthiness analysis of thin-walled bio-inspired multi-cell corrugated tubes under quasi-static axial loading [J]. Engineering Structures, 2020, 204: 110069.

[8] Sun G, Pang T, Fang J, et al. Parameterization of criss-cross configurations for multiobjective crashworthiness optimization [J]. International Journal of Mechanical Sciences, 2017, 124-125: 145-57.

[9] Chen W, Wierzbicki T. Relative merits of single-cell, multi-cell and foam-filled thin-walled structures in energy absorption [J]. Thin-Walled Structures, 2001, 39(4): 287-306.

[10] Zhang X, Zhang H. Theoretical and numerical investigation on the crush resistance of rhombic and kagome honeycombs [J]. Composite Structures, 2013, 96: 143-52